



ELSEVIER

Available online at [www.sciencedirect.com](http://www.sciencedirect.com)

SCIENCE @ DIRECT®

Physica C 388–389 (2003) 731–732

PHYSICA C

[www.elsevier.com/locate/physc](http://www.elsevier.com/locate/physc)

## Dynamics of the second magnetization peak in $\text{Bi}_2\text{Sr}_2\text{CaCu}_2\text{O}_{8+\delta}$

D. Giller, B. Kalisky, I. Shapiro, B. Ya. Shapiro, A. Shaulov, Y. Yeshurun \*

*Institute of Superconductivity, Bar-Ilan University, Ramat-Gan 52900, Israel*

### Abstract

Local magnetization curves at different times, extracted from high-temporal resolution magneto-optical measurements in  $\text{Bi}_2\text{Sr}_2\text{CaCu}_2\text{O}_{8+\delta}$ , demonstrate the absence of the second magnetization peak (SMP) at short times, its appearance at longer times, and the movement of its onset toward higher induction fields approaching the limit of the thermodynamic order–disorder transition field. We utilize theoretical analysis, based on the Landau–Khalatnikov dynamic equation adopted for the vortex matter order parameter, to simulate the measured time evolution of the SMP. We show that the observed time evolution is a manifestation of a dynamic coexistence of transient-disordered and ordered vortex phases.

© 2003 Elsevier Science B.V. All rights reserved.

*Keywords:* Fishtail; Second peak; Magneto-optics; Flux lines;  $\text{Bi}_2\text{Sr}_2\text{CaCu}_2\text{O}_{8+\delta}$ ; Vortex phase transitions; Phase dynamics

The mystery of the dynamic behavior of the second magnetization peak (SMP) in  $\text{Bi}_2\text{Sr}_2\text{CaCu}_2\text{O}_{8+\delta}$  (BSCCO) has been a subject of several works (see, e.g., [1,2]). In Fig. 1 we demonstrate the details of this effect as manifested in magneto-optical (MO) measurements. The measurements were performed on a  $1.55 \times 1.25 \times 0.05 \text{ mm}^3$  BSCCO single crystal ( $T_c \sim 92 \text{ K}$ ) at  $T = 22.5 \text{ K}$ . The external magnetic field was raised abruptly (rise-time  $< 50 \text{ ms}$ ) from zero to a target value  $H$  between 140 and 430 Oe, and from  $H=430$  to a target value  $H$  between 430 and 840 Oe with a constant step of 430 Oe. Immediately after the field change, MO images were recorded at time intervals of 40 ms for 30 s. From these images, local  $\text{dB}/\text{dx}$  vs.  $B$  curves were derived for different times. It is clear from the figure that the SMP is absent at short times, it starts to develop at approximately  $t = 0.16 \text{ s}$ , and its onset (marked by arrows in Fig. 1) moves with time toward higher fields. Similar results were observed by, e.g., Yeshurun et al. [1] in their global (squid) measurements and Konczykowski et al.

[2] exploiting a Hall probe array. These dynamic phenomena were previously explained, in the framework of the collective creep theory, associating the SMP with a crossover among different creep mechanisms [1,3–5]. However, later works [6–9] demonstrated that the SMP in BSCCO is a consequence of a sharp (possibly first order) thermodynamic vortex phase transition. Thus, the origin of the dynamic phenomena related to the SMP requires further explanation.

We discuss here a mechanism for the creation of the SMP and present numerical calculations simulating the dynamics of the SMP phenomenon. The discussion is based on our recent observation of transient vortex states in which disordered and ordered vortex phases coexist dynamically, with a sharp border between them [7,10]. Our high spatial resolution MO setup allows identification and tracing the movement of this border. By correlating the induction profiles at a given time with the  $\text{dB}/\text{dx}$  vs.  $B$  curve at the same time, we find that the induction at the border between the two phases signifies the onset induction of the sharp increase in  $\text{dB}/\text{dx}$ .

Based on the accumulated data, the scenario of the “dynamic SMP” is as follows. At short times, immediately after a change in the field, the vortices are in a

\* Corresponding author.

E-mail address: [yeshurun@mail.biu.ac.il](mailto:yeshurun@mail.biu.ac.il) (Y. Yeshurun).

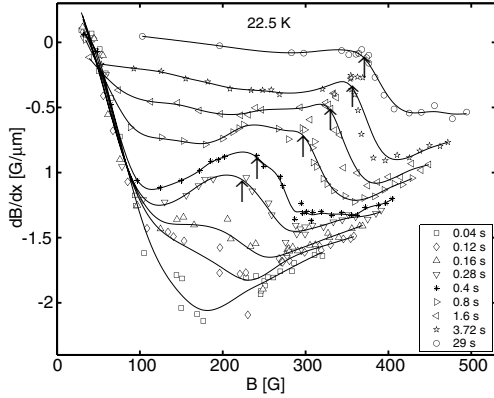
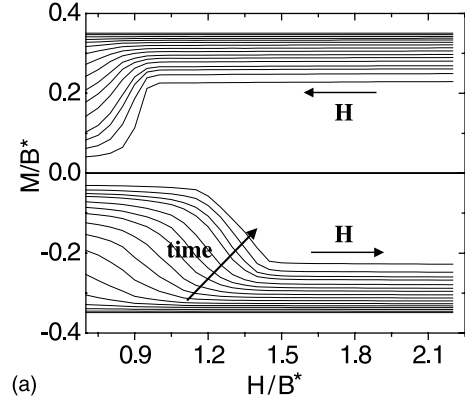


Fig. 1. Local curves  $dB/dx$  vs.  $B$  for different time windows, mapped from measured time evolution of induction profiles.

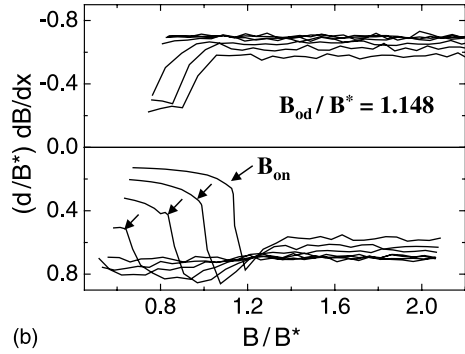
transient-disordered (TD) phase in the whole sample. As a result, the SMP is absent. As time elapses, the ordered phase nucleates near the sample center where the field is minimal [10], creating a border between the TD and the ordered vortex phases. As a result, the onset of the SMP (dip in  $dB/dx$  vs.  $B$ ) starts to develop at low fields. As the border moves toward the sample edges, the induction at the border increases and, as a result, the SMP onset also increases. Obviously, the onset induction cannot exceed the order–disorder transition induction  $B_{od}$ , as above  $B_{od}$  the growth of the ordered state is halted and the whole sample is in a disordered state [7].

The above process can be fully described by the Landau–Khalatnikov (LK) dynamic equation  $\partial\Psi/\partial t = -\Gamma\delta F/\delta\Psi$  [10], where  $\Psi$  is the order parameter,  $\Gamma$  is the LK damping coefficient,  $F = D(\nabla\Psi)^2/2 - \alpha\Psi^2/2 - \beta\Psi^3/3 + \gamma\Psi^4/4$  is the free energy functional of the system,  $\alpha = (1 - B/B^*)$ ,  $\beta$ ,  $\gamma$ ,  $D$  are the Landau coefficients, and  $B^*$  is the field of the lower limit of metastability. Different creep characteristics of the ordered and TD phases are taken into account by adopting the experimentally known  $E(j)$  curves:  $E_1(j) \sim j^{1.9}$  and  $E_2(j) \sim j^3$  [11]. Matching the  $E(j)$  curves at the border between the two phases yields:  $E(j, \Psi) = E_1(j)[\Psi/\Psi_0]^v + E_2(j)[1 - \Psi/\Psi_0]^v$ , where  $\Psi_0$  is the value of the order parameter in an equilibrium ordered phase (in the TD phase  $\Psi = 0$ ) and  $v$  is a power of order 1. Other numerical parameters are similar to those taken in [10].

We solve numerically the above equations, together with the Maxwell equations  $c\nabla \times \vec{B} = 4\pi\vec{j}$  and  $c\nabla \times \vec{E} = -d\vec{B}/dt$ , for a slab geometry, at different applied fields  $H$  and different times. The derived global magnetic moment,  $M(H) = \int(B - H) dx$ , and local gradient of the magnetic induction  $dB/dx(B)$  at distance  $x/d = 0.8$  from the sample center ( $d$  is the half-width of the sample), are shown in Fig. 2(a) and (b), respectively, for different times. We note the similarity between the calculated and experimental results. In particular, the SMP is absent at



(a)



(b)

Fig. 2. Numerical calculation of (a) global magnetic moment  $M(H)$  and (b) local  $dB/dx(B)$  for different times. Arrows in (b) point to the onset of the SMP at  $B_{on}$ .

short times, it appears at later times, and the onset field increases with time toward  $B_{od}$ .

## Acknowledgements

We thank T. Tamegai for providing the BSCCO crystal. A.S. acknowledges support from the Israel Science foundation. This research is supported by The Israel Science Foundation—Center of Excellence Program, and by the Heinrich Hertz Minerva Center for High Temperature Superconductivity.

## References

- [1] Y. Yeshurun et al., Phys. Rev. B 49 (1994) 1548.
- [2] M. Konczykowski et al., Physica C 341 (2000) 1317.
- [3] L. Krusin-Elbaum et al., Phys. Rev. Lett. 69 (1992) 2280.
- [4] G. Blatter et al., Rev. Mod. Phys. 66 (1994) 1125.
- [5] L. Burlachkov et al., Phys. Rev. B 58 (1998) 15067.
- [6] B. Khaykovich et al., Phys. Rev. Lett. 76 (1996) 2555.
- [7] D. Giller et al., Phys. Rev. Lett. 84 (2000) 3698.
- [8] C.J. van der Beek et al., Phys. Rev. Lett. 84 (2000) 4196.
- [9] N. Avraham et al., Nature 411 (2001) 451.
- [10] D. Giller et al., Phys. Rev. B 63 (2001) R220502.
- [11] D. Giller, Ph.D. thesis, Bar-Ilan University, Israel, 2002.